



Elliptic neutron-focusing supermirror for illuminating small samples in neutron reflectometry

TAKUYA HOSOBATA,^{1,*} NORIFUMI L. YAMADA,² MASAHIRO HINO,³ HISAO YOSHINAGA,³ FUMIYA NEMOTO,² KOICHIRO HORI,^{2,4} TOSHIHIDE KAWAI,¹ YUTAKA YAMAGATA,¹ MASAHIRO TAKEDA,¹ AND SHIN TAKEDA¹

¹RIKEN Center for Advanced Photonics, RIKEN, 2-1 Hirosawa, Wako, Saitama 351-0198, Japan

²Neutron Science Division, High Energy Accelerator Research Organization (KEK), 203-1 Shirakata, Tokai, Naka, Ibaraki 319-1106, Japan

³Institute for Integrated Radiation and Nuclear Science, Kyoto University, 2 Asahiro-Nishi, Kumatori, Sennan, Osaka 590-0494, Japan

⁴Sumitomo Rubber Industries, LTD., 3-6-9 Wakino-hama-cho, Chuo-ku, Kobe, Hyogo 651-0072, Japan

*takuya.hosobata@riken.jp

Abstract: This paper details the development of a precise assembly of two supermirrors for neutron-focusing, designed for installation in neutron reflectometer SOFIA at BL16 in J-PARC MLF to intensify the illumination for small samples. The supermirrors are sputtered on two metal substrates, whose surfaces are coated with amorphous Ni-P plating, and are figured by diamond cutting and polished to subnanometer roughness. Special care is taken while polishing the substrates to reduce waviness and surface roughness for achieving a sharp focusing spot and uniform neutron reflectivity. The supermirror could converge the neutrons into a focal spot with a width of 0.13 mm in the full width at half maximum.

© 2019 Optical Society of America under the terms of the [OSA Open Access Publishing Agreement](#)

1. Introduction

As guides that transport neutrons from moderators to instruments, neutron supermirrors: multilayers that achromatically reflect slow neutrons at large critical angles, are indispensable in neutron research facilities. The supermirrors used in neutron guides are generally deposited on flat substrates, which are then assembled to form rectangular tubes. Slight bending of these supermirrors on the tubular walls appends extra functions to the guide tubes, such as neutron transport with fewer reflections and neutron intensification after exiting the tube while increasing the beam divergence. As an extension of this common usage, there is a demand for the application of supermirrors as precise focusing devices. Such focusing mirrors bring innovations to neutron instruments, e.g., in mapping measured quantities by localized illumination on the sample, and downsizing small-angle neutron scattering instruments by focusing on detectors. However, because neutron-focusing supermirrors originate from neutron guides, their development has been based on the assumption that the substrates are flat, limiting the focusing precision; hence, the technologies for developing neutron-focusing supermirrors on figured substrates remain immature. To promote further development, we report the successful production of a neutron-focusing supermirror designed for permanent installation in a neutron reflectometer, in this study. The objective is to provide the methods and criteria for preparing substrates for the supermirror in order to upgrade neutron instruments by introducing high-precision focusing optics.

For a supermirror to function as a focusing device, its slope distribution must be appropriate for directing the neutrons reflected at all positions toward the focus. One approach to realize such slope distribution is to bend the supermirror deposited on a flat substrate, typically float

glass or silicon wafer; focusing devices based on this concept have been reported [1–3]. The greatest advantage of bent mirrors is the ease of supermirror deposition because deposition using sputtering machines is well established for flat substrates. Another advantage is the adjustability of the curvature; focusing supermirrors with adjustable focal lengths are being developed [4–7]. Despite these advantages, there are two problems in bent mirrors: First is that the realizable forms are limited. As substrates can be bent in only one direction, axisymmetric forms for high-gain two-dimensional focusing such as ellipsoids and paraboloids cannot be realized. This limits the options for the two-dimensional focusing to the combinations of bent mirrors: Kirkpatrick-Baez and Montel mirrors. Secondly, the attainable form accuracy is limited because the surface curvature is governed by the elasticity. This renders bent mirrors unsuitable for applications requiring long focal-length in which slight slope errors deflect neutrons from the focus by a large distance.

To realize precise neutron-focusing supermirrors in various forms, supermirrors must be deposited on substrates with figured surfaces. However, the production of such substrates is difficult even with the state-of-the-art optics fabrication technology because the prerequisite form accuracy and smoothness for supermirrors are considerably more demanding than those for common optics. Despite these difficulties, successful production of elliptic supermirrors has been reported using precisely figured glass substrates [8–10]. Similar supermirrors with figured substrates have been reported by the authors, in which Ni-P plated aluminum was chosen as a substrate material over glass and silicon, for good machinability and radiation resistance [11,12].

In this paper, we describe the development of a neutron-focusing supermirror in detail for a neutron reflectometer named SOFIA located at BL16 in the Japan proton accelerator research complex, materials and life science experimental facility (J-PARC MLF) [13,14]. The supermirror is elliptic, curved only in one direction for one-dimensional focusing. This focusing supermirror is introduced for intensifying the neutron illumination for small samples to improve the efficiency of the experiments for the effective utilization of the limited beam time. For this application, there are three challenges in substrate production, as mentioned below:

- a). High accuracy is required due to the long focal-length. The length of the semimajor axis exceeds 2 m and the desired focal-spot size is 0.1 mm, indicating that the slope error must be maintained within tens of microradians.
- b). A large area is required for maintaining the neutron divergence as large as possible for intensity gain. The required size of the supermirror exceeds the capability of most sputtering machines. Therefore, segments of the supermirror on separate substrates need to be precisely assembled to form a single surface.
- c). The supermirror segments must be identical with respect to the neutron reflectivity for avoiding biased illumination. For uniformity, the substrates need to be polished to an extent where their roughness have no influence on the reflectivity of the supermirror.

Our previous works on the development of neutron-focusing supermirrors have been devoted to these problems [11,12]. Although we have made steady progress in each work, the fabricated supermirrors were insufficient for practical use. In contrast, the supermirror described in this paper is definitive with sufficient focusing performance for permanent installation in SOFIA; this is realized by improving the polishing and assembly of the substrates. Thus, the following details on this supermirror development can be a useful reference for optics developers and instrument scientists, who can contribute to the advancement of neutron instrumentation.

2. Focusing-supermirror for neutron reflectometry

Figure 1 shows the neutron-focusing supermirror designed to enhance the performance of neutron reflectometer SOFIA at BL16 in J-PARC MLF. The supermirror is a multilayer composed of

NiC/Ti bilayers deposited on two metallic substrates. The number of bilayers is 210 and the thickness of the bilayers change gradually along the depth; the thickness of NiC and Ti layers range from 5.08–60 nm and 4.76–13.1 nm, respectively. This multilayer is designed such that the critical angle of total reflection becomes thrice that of pure nickel. The surfaces of the two substrates form a single ellipse when assembled. The ellipse is designed such that the diverged neutron beam from the source slit at one of the foci is reflected by the supermirror and converges at the sample located at the other focus. The length of the major axis is 4.3 m and the ratio of the major to the minor axis is 100 : 1. This ratio represents the specified incident angle of the neutron beam on the mirror, 10 mrad.

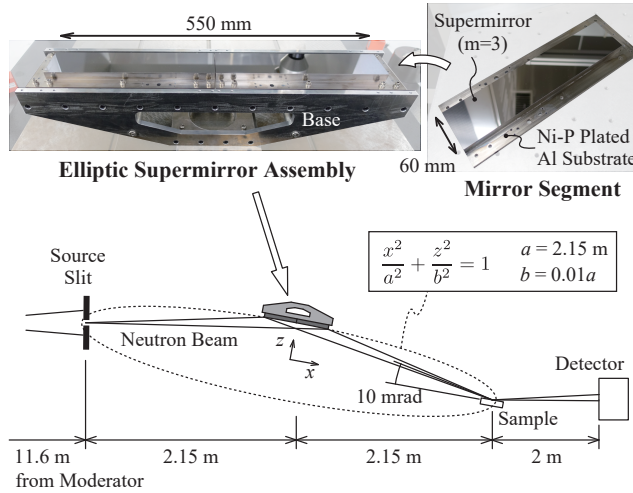


Fig. 1. Designed geometrical values of the elliptic neutron-focusing supermirror on a metal substrate assembly for neutron reflectometer SOFIA at BL16 in J-PARC MLF.

The aim of introducing this focusing supermirror is to enable efficient neutron reflectivity measurements of small samples measured using X-ray reflectometry. This is based on our conviction that the compatibility of the sample sizes between these complimentary reflectivity measurements is important. We aim to illuminate 10 mm-long samples along the beam traveling direction, which is the typical sample size for X-ray reflectivity measurements. To illuminate this sample area with the typical incident angle for neutron reflectivity measurements, i.e. 10 mrad, a beam size of 0.1 mm should be achieved at the sample position because it is elongated 100 times on the sample surface. It has been demonstrated that illumination by such a focused beam results in more neutron intensity compared to conventional multislit collimation, improving the time-efficiency of neutron reflectometry [11,15,16]. Note that in the neutron reflectometry using focused beam, the beam divergence at the sample will be wider than in the conventional method that collimates the beam using two slits. For this reason, data correction for the variance of incidence angle is required; this is easily performed as long as position sensitive detectors are used.

This neutron-focusing system has two types of intrinsic optical aberrations, which we chose to tolerate. The first aberration is the chromatic aberration due to the gravity. The gravity deflects neutrons from the focus and this is more prominent for slower neutrons because they have longer time of flight. In SOFIA, available wavelengths of neutrons range from 0.2–0.88 nm, with the intensity peak at 0.26 nm. Majority of the neutrons with short wavelengths are fast enough such that the broadening of focal spot by the gravity is within a few micrometers. In contrast, the slowest neutrons with 0.88 nm wavelengths are deflected from the focus by approximately 30 μm . However, this effect is negligible because the number of such slow neutrons are less by

two to three orders of magnitude compared to the neutrons at the intensity peak. The second aberration is the coma aberration due to the finite size of the virtual source, i.e. the slit. This effect is inevitable in focusing systems with a single elliptic mirror, and the effect becomes worse as the length of the focusing mirror becomes longer. We could tolerate this because the focusing mirror is rather short, and the broadening of the focal spot by coma aberration is limited to approximately 30 % of the slit width. To incorporate longer mirrors, measures must be taken to cancel such coma aberration, e.g. by using a series of elliptic mirrors as demonstrated in a neutron reflectometer Amor at Paul Scherrer Institut [15].

3. Refinements in the neutron-focusing supermirror

The neutron-focusing supermirror in this work is a refined version of the mirror described in [12]. The fabrication process is illustrated in Fig. 2. The substrates are figured by diamond cutting, smoothened by polishing, coated with the supermirror, and are then assembled to form a single surface. The originality of the supermirror is that the substrates are composed of metals alone, and can therefore be easily machined to free-form surfaces. The substrate for the supermirror is composed of aluminum primarily alloyed with magnesium (A5052), covered with an amorphous phosphorous-rich nickel (Ni-P) plating. The former allows easy free-forming, while the latter provides the subnanometer surface roughness required for supermirror deposition.

There are three differences between the newly developed mirror and the previous one with respect to substrate production, as follows:

1. The waviness is reduced by improving the polishing method for sharpening the focal spot.
2. The surface roughness is reduced by longer polishing for high and uniform neutron reflectivity.
3. The fixtures are rigidified for a robust assembly.

The first two are refinements to improve the performance of the neutron focusing mirror, whereas, the third is more of a compromise; in precision assembly, a trade-off exists between the precision and robustness, and the latter is selected for this application. The details on each of these three refinements are given below.

3.1. Polishing method for reducing waviness

Waviness, which is the figure error with respect to an ideal ellipse with a short spatial period, degrades the focusing performance of the mirror because the spatially periodic slope error it causes broadens the focal spot. In our previous mirror, the waviness in the spatial frequency band from $0.2\text{--}2 \text{ mm}^{-1}$ was the main cause of focal-spot broadening. Waviness is caused by the deviation of the cutting tool during the figuring process, and its amplitude is of the order of 10–100 nm. Such deviation cannot be eradicated, even with cutting-edge ultraprecision machines. Hence, we removed the waviness by polishing, which serves as a low-pass filter in surface processing.

For our previous supermirror, the substrates were polished in two steps: rough polishing to remove the tool marks from the figuring process and fine polishing to achieve sub-nm roughness that is a prerequisite for sputtering supermirrors. For this polishing, a small disk-like polishing pad with a diameter of 20 mm was scanned on the surface of the substrate, while rotating at 3000 rpm, and pressed against the substrate at a pressure of 3 kPa. During scanning, polishing slurry was constantly applied to the interface between the pad and substrate. The removal characteristic of such polishing in terms of the spatial frequency is determined by the hardness of the polishing pad and the abrasives. For both rough and fine polishing, we used soft suede pads. The abrasives in the polishing slurry were alumina (grain size: 300 nm) and colloidal silica (particle diameter:

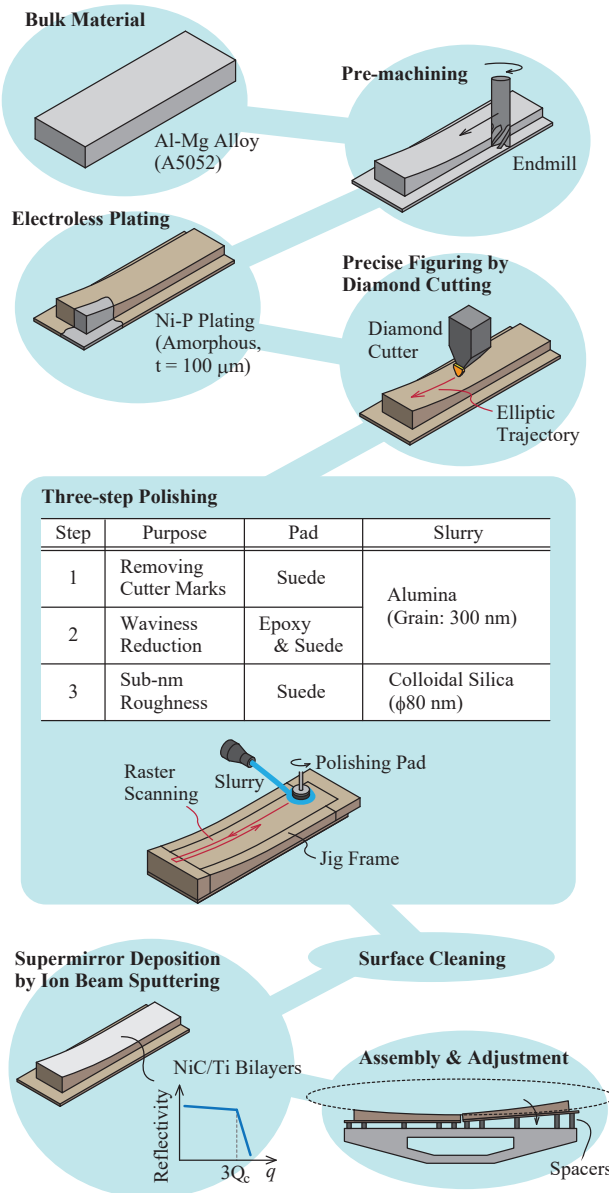


Fig. 2. Fabrication process of the neutron-focusing supermirror assembly on metal substrates.

80 nm), respectively, for rough and fine polishing. The results of our previous mirror indicated that waviness ranging from $0.2\text{--}2 \text{ mm}^{-1}$ in the spatial frequencies cannot be removed by these processes.

In this work, to remove waviness, we included another step between the rough and the fine polishing steps. For this corrective polishing, we used a polishing pad made of epoxy, which is considerably harder than the suede pad, along with alumina slurry. This was selected because harder polishing pads tend to remove the waviness at low spatial frequencies, as demonstrated for glass substrates [8]. Although polishing using epoxy pad was successful in reducing waviness, it

posed another problem, in which too much polishing formed a nonuniform dapple-like pattern on the surface. This may be due to the unevenness of the polishing pressure caused by the stiffness of the polishing pad. To prevent the formation of this dapple-like pattern, we used a hard epoxy pad and soft suede pad, and polished alternately.

Figures 3(a) and 3(b) depict the change in the slope error, from the as-cut by diamond cutting to after corrective polishing. The large amplitude waviness in the as-cut state was reduced by rough polishing using the soft pad, but the waviness ceased to decrease after approximately 20 h. Corrective polishing was then applied, which involved 4 h of polishing using the hard epoxy pad and 4 h of the polishing using the soft suede pad, alternately. In this case we performed six rounds of corrective polishing; a drastic decrease in the waviness was observed. Figure 4 displays the power spectrum density diagram of the slope errors in each of these states. This indicates that corrective polishing can efficiently reduce the waviness in a wide spatial frequency band, in contrast to the rough polishing that reduces the waviness only at high spatial frequencies. As described in Section 4., the focusing supermirror deposited on substrates with less waviness is capable of converging neutrons to a sharp spot.

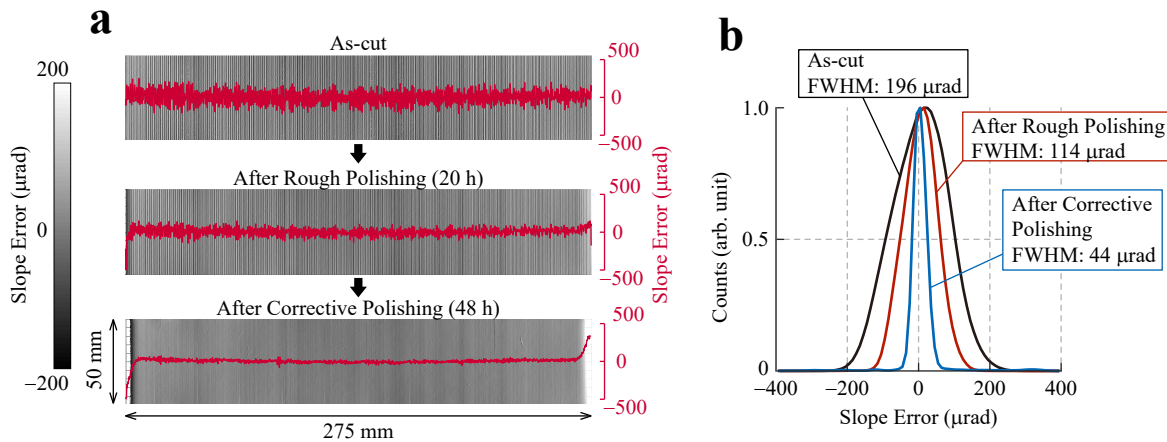


Fig. 3. Decrease in the waviness of the substrate surface by rough and corrective polishing: (a) gray-scale images showing the maps of the longitudinal slope errors with the red lines showing their cross-sections along the center line, and (b) the frequency distribution of the slope error. The maps are obtained by stitching from multiple maps measured using a laser interferometer (Verifier QPZ, Zygo Corp.). The slope errors are relative to the best-fit ellipse, whose lengths of the semimajor and semiminor axes are 2050 mm and 21.5 mm, respectively. Note that at these states, the substrate is slightly deformed because it is fixed to the polishing frame for polishing near edges.

3.2. Extra polishing for uniform roughness

Besides the broadened focal spot caused by waviness, another problem in our previous mirror was the difference in the neutron reflectivities of the supermirrors on the two substrates; at the critical angle of total reflection, the reflectivity differed by 22 % [12]. The supermirrors themselves did not cause this difference because they were sputtered on the two substrates simultaneously at exactly the same condition. Hence, this difference was due to the surface roughness of substrates because the two substrates were polished one at a time due to the size restriction of the polishing machine. Although the surface roughness of the two substrates appeared to be identical at approximately 0.2 nm(rms) when measured with a white-light scanning interferometer (NewView 7200, Zygo), it is probable that the difference was below the spatial resolution of the interferometer, which was 0.22 μm .

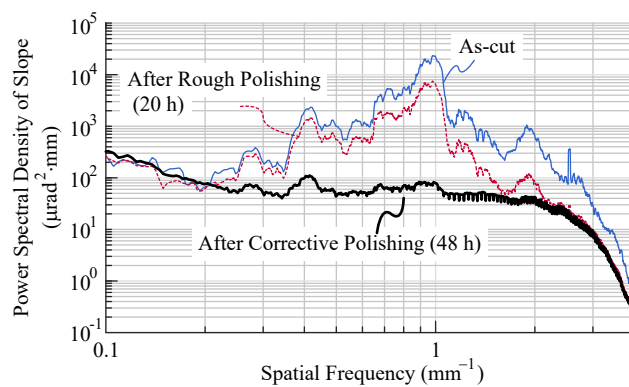


Fig. 4. Power spectral density of the longitudinal slope error of the supermirror substrate at each production phase. The data were obtained using a laser interferometer (Verifier QPZ, Zygo Corp.).

To overcome the above-mentioned problem, we decided to perform fine polishing for more time; we continued to polish until there were no more changes on the substrate surface. Such an approach is effective in homogenizing the surface roughness of the two substrates because the substrates cannot be polished beyond the capability of the abrasive used in the finishing process, namely colloidal silica. Besides the type of the abrasive, the polishing condition was the same for rough polishing using the soft suede pad.

Figure 5(a) shows the surface roughness of the substrate before and after 32 h of fine polishing. At the initial condition, the roughness is approximately 2 nm(rms), which is the roughness limit that can be achieved by the preceding process using alumina slurry. After fine polishing using colloidal silica, the roughness was reduced to 0.1 nm(rms). Figure 5(b) shows the reduction in the surface roughness with the progress of polishing. The roughness decreases exponentially and converges to 0.1 nm(rms), which is close to the lower bound of the roughness that can be measured by the white-light scanning interferometer. In addition to the magnitude of the roughness, the error bars representing the position dependence are crucial; the short error bars at the final state indicate that the roughness varies mainly because of measurement noise.

This result provides a criterion for polishing substrates: the substrates need to be polished beyond the capability of white-light scanning interferometers. This criterion is supported by the uniform neutron reflectivity obtained using supermirrors on such substrates, as demonstrated in Sec. 4. Note that these supermirrors were deposited at the ion-beam sputtering facility at the Institute for Integrated Radiation and Nuclear Science at Kyoto University (KURNS) [17].

3.3. Assembly and alignment by precise spacer adjustment

In the previous mirror, we adopted kinematic couplings as fixtures for assembling the supermirror segments [12], which enabled us to fix and adjust the segments with minimal stress and deformation. However, as we continued with the development, we occasionally encountered a problem in transportation. Although the two mirror segments were precisely aligned at RIKEN, they were misaligned by vibration while transporting to J-PARC, located 120 km away. This demonstrates the trade-off often encountered in precision assembly: satisfying the robustness against inertial load as well as obtaining precise adjustability is a difficult design problem. A possible solution is to realign the supermirrors near the beamline; however, it is unrealistic because such precise alignment requires a large-sized profilometer.

To ensure the invariance of the supermirror assembly before and after transportation, we abandoned the kinematic couplings and decided to bolt-fix the segments onto a bridge-like base

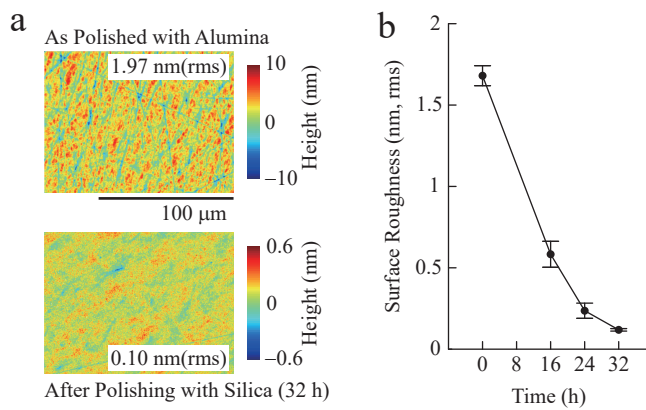


Fig. 5. Surface roughness of the supermirror substrate: (a) surface roughness before and after 32 h of polishing with colloidal silica and (b) reduction in the roughness with time. The error bars represent the standard deviation of the roughness in nine different positions. The roughness was measured with a white-light scanning interferometer (NewView7200, Zygo Corp.).

structure, as shown in Fig. 6. Generally, direct fixing with bolts is avoided for optical elements because the bolt stress ruins their optical functions by surface deformation. However, this was not applicable for our mirror because we used metallic substrates with thin flanges surrounding the optical surface. These flanges serve as buffers, preventing the supermirror-coated optical surfaces from deformation. This demonstrates the design freedom offered by metallic substrates, which is a significant advantage over glass- and silicon-based substrates.

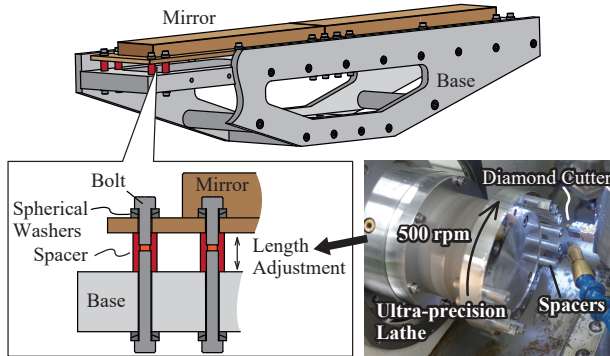


Fig. 6. Rigid fixturing of the supermirror segments onto the base structure. The lengths of the intervening spacers are precisely adjusted using an ultraprecision lathe (ULG-100A, Toshiba Machine Co., Ltd.)

To align the two bolt-fixed supermirror segments to form a single elliptical surface, we inserted spacer rods between the segments and the base structure. The lengths of these spacers were adjusted based on the form measurement to reduce the relative translational/angular displacement and the twists of each segment as well. For adjusting the spacer lengths, we performed diamond turning using an ultraprecision lathe (ULG-100A, Toshiba Machine Co., Ltd.) with a positioning resolution of 10 nm. Form measurement was performed using a coordinate measurement machine (Legex, Mitutoyo Co., Ltd.) equipped with a laser autofocus probe (PFU-3, Mitaka Kohki Co., Ltd). The result of this adjustment is depicted in Fig. 7. The relative lengths of the spacers

in each round of adjustment indicate that the spacers must be adjusted with a precision of few micrometers. After three rounds of measuring and adjusting, the relative angular displacement of the two supermirror segments was below $1 \mu\text{rad}$. Note that there is an in-plane gap between the two supermirror segments to prevent the segments from interfering during adjustment. The gap is an ineffective area of the supermirror, through which the neutrons pass through. However, its effect in focusing is negligibly small, because the length of the gap is approximately 1 mm, much shorter than the length of the whole mirror.

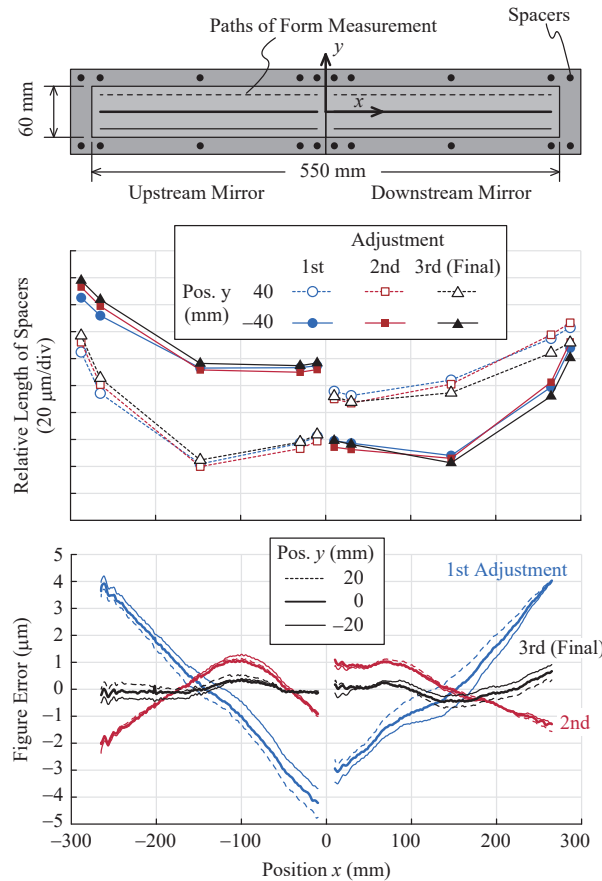


Fig. 7. Alignment of the supermirror segments to form a single elliptical surface by adjusting the spacer lengths. The form is measured using a coordinate measurement machine (Legex, Mitutoyo Co., Ltd.) equipped with a laser autofocus probe (PFU-3, Mitaka Kohki Co., Ltd). Note that the figure errors are relative to the best-fit ellipse. The lengths of the semimajor and semiminor axes of the ellipse are 2219 mm and 21.5 mm, respectively.

3.4. Summary of the final assembly

The precision of the final supermirror segment assembly is summarized in Figs. 8(a) and 8(b). As shown in Fig. 8(a), the figure error with respect to the best-fit ellipse is $2.5 \mu\text{m(P-V)}$, which is mostly due to the deformation of the downstream segment. Such deformation can be resolved by more adjustment trials, which we could not perform due to time restriction. Figure 8(b) shows the slope error distribution along the center line of the mirror. This is one of the critical qualities of the focusing supermirror because it determines the minimal size of the focal spot. The full width

at half maximum (FWHM) of the slope error of the upstream segment is $23.7 \mu\text{rad}$, whereas that of the deformed downstream segment is $33.6 \mu\text{rad}$. As a result, the FWHM of the slope error of the assembly of the two supermirrors is $27.7 \mu\text{rad}$. The slope error $\Delta\theta$ deflects the neutrons from the focus by a distance $2L\Delta\theta$, where L is the distance from which the neutron is reflected to the focus. Hence, if we assume $L = 2.15 \text{ m}$ for approximate estimation, the focal spot size is estimated to be $0.12 \text{ mm}(\text{FWHM})$, which agrees well with the experimental result in the next section.

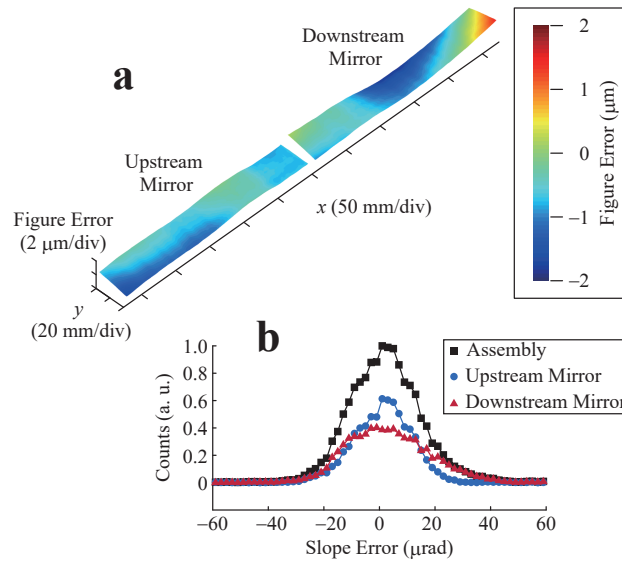


Fig. 8. Summary of the elliptic neutron-focusing supermirror precision: (a) figure error with respect to the best-fit ellipse, measured by an interferometer (Verifier QPZ, Zyglo Corp.) and (b) longitudinal slope error distribution along the center line. The lengths of the semimajor and semiminor axes of the best-fit ellipse are 2219 mm and 21.5 mm , respectively.

4. Results of neutron experiments

We performed two experiments with SOFIA to evaluate the quality of the refined neutron-focusing supermirror. The first experiment involved reflectivity measurement, whereas the second involved the characterization of the mirror's focusing performance.

4.1. Reflectivity measurement

Figure 9 shows the geometry for the reflectivity measurement. The mirror was placed on the sample stage with the mirror-side facing up and the longitudinal direction perpendicular to the neutron beam, to avoid the influence of the curvature of the elliptic surface. The incident beam was collimated by two slits, S1 and S2, such that the illuminating footprint was $25 \times 20 \text{ mm}^2$. The angle of reflection θ was determined by comparing the positions of the reflected beam (with the mirror) and direct beam (without the mirror), detected by a two-dimensional ${}^6\text{LiF}/\text{ZnS}$ scintillation counter. The wavelengths λ of the detected neutrons were calculated using the time-of-flight method. Finally, the neutron reflectivity was calculated as the ratio of the direct and reflected neutron counts for each momentum transfer ($q = 4\pi \sin \theta/\lambda$).

An example of the measured neutron reflectivity is shown in Fig. 10(a). The momentum transfer at the critical angle of total reflection is $q_c = 0.63 \text{ nm}^{-1}$. Supermirrors are classified by the value m defined as $m = q_c/Q_c$, where $Q_c = 0.217 \text{ nm}^{-1}$ is the critical momentum transfer for

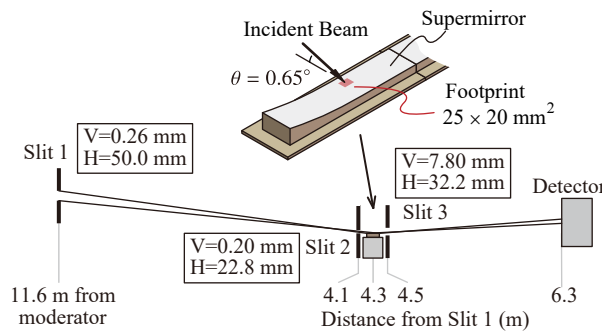


Fig. 9. Geometry for the neutron reflectivity measurement of the supermirror. The vertical and horizontal slit widths are denoted by V and H, respectively.

pure nickel. Thus, the reflectivity curve indicates that the supermirror is an $m = 2.9$ supermirror. In the same graph, the reflectivity of the supermirror on a silicon wafer, sputtered in the same batch as the focusing supermirror, is shown for comparison. The reflectivity curves are identical indicating that the polished metal substrates have equivalent surface roughness as the silicon wafer. The reflectivity was measured at 40 different locations on the mirror, and the reflectivity at the critical momentum transfer (q_c) for each location is depicted in Fig. 10(b). The reflectivity at the critical condition is $86.2 \pm 2.5(\sigma)$ % for all the locations; thus, the two supermirror segments can be considered to have identical and position-independent neutron reflectivity.

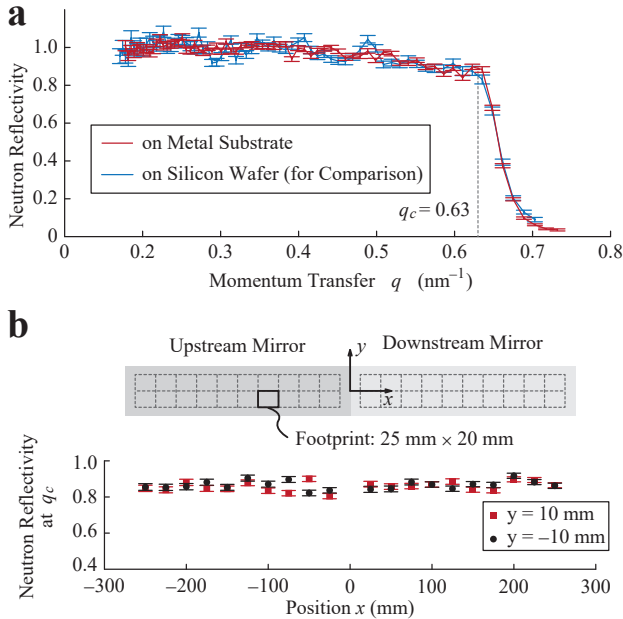


Fig. 10. Neutron reflectivity of the focusing supermirror: (a) reflectivity curve at $(x, y) = (200, -10)$ mm and (b) reflectivity at the critical momentum transfer q_c . The reflectivity curve of the supermirror on a silicon wafer is also shown for comparison. Note that q_c is $0.628 \pm 0.007(\sigma) \text{ nm}^{-1}$ for all the positions.

4.2. Focusing experiment

The supermirror was installed in SOFIA, as depicted in Fig. 1, for testing its neutron-focusing performance. The mirror was mounted on a stage with which the vertical position and tilt angle can be varied for optical alignment. To measure the vertical distribution of the neutrons passing the sample position, a cadmium slit with a $5\ \mu\text{m}$ opening was placed on the sample stage. The sample stage carrying the slit was moved in the vertical direction, and the neutrons that passed through the slit were counted using a scintillation counter. Hence, the neutron counts plotted against the slit position represent the profile of the focal spot, i.e. the vertical distribution of the neutron intensity at the sample position.

The measured profile of the focal spot of the new supermirror is depicted in Fig. 11. For comparison, the profiles of the previous supermirror in [12] and a single segment of the new supermirror are also displayed. Compared to the previous supermirror, the neutron intensity increased significantly near the peak, while the intensity in the tails beside the peak decreased; the Lorentzian-like distribution became a sharper Gaussian-like distribution, which is more favorable for a focusing device. The FWHM of the Gaussian profile was $0.129\ \text{mm}$, which agrees well with the prediction based on the slope error distribution. The sharpened spot is mainly due to the reduction in the waviness, and partly due to the decreased diffuse scattering due to the reduction in the surface roughness. However, the focusing performance of the assembled supermirror was inferior to the case with a single supermirror segment, which has an FWHM of $0.08\ \text{mm}$. This indicates that the present neutron-focusing supermirror has a room for improvement with respect to the assembly precision.

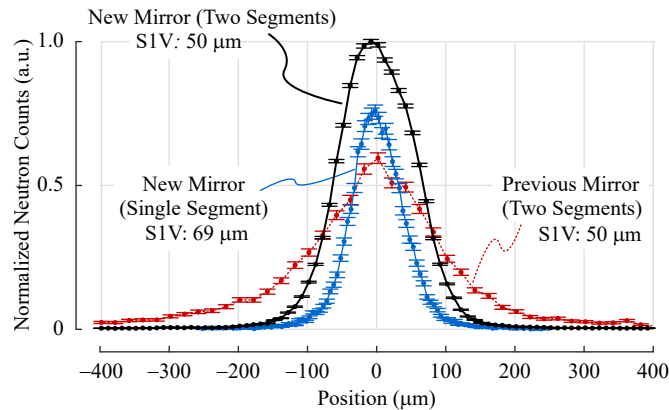


Fig. 11. Vertical distribution of the neutron beam at the focus of the neutron-focusing supermirror. S1V represents the vertical width of the source slit during the experiment. Note that the neutron counts are normalized such that the total neutron count is proportional to the area of the supermirror.

5. Discussion

The results of this work suggest two points of practical importance for future developers of neutron-focusing optics. First is that the focusing performance of a neutron supermirror can be precisely predicted before the actual neutron experiments, based on the slope error measured using laser interferometers. Moreover, this implies that the level to which the waviness should be reduced is known, in order to satisfy the requirement of the neutron instrument. Next, for the supermirror to have uniform neutron reflectivity, the substrate should be polished to an extent where the surface roughness approaches the measurable limit of white-light scanning interferometers. This criterion is not physically essential but is practically useful because

atomic force microscopes that gauge the roughness with higher spatial resolution are often inapplicable to large substrates which are required for focusing supermirrors. Thus, although the neutron-focusing supermirror in this work is developed for a specific neutron reflectometer, the knowledge obtained during development has universal value.

The precise assembly of the supermirror is a challenge for future. As previously mentioned, the trade-off between the precision and robustness of the optical assembly complicates the design problem of realizing focusing supermirrors with large area. For finer focusing, a simple but expensive solution is to actively control the relative positions and angles of each supermirror segment such that the alignment can be done onsite at the neutron beamlines. However, the assembly method proposed in this work is sufficient for most applications whose focal length and/or spot size requirements are less stringent than those of SOFIA.

This work establishes a production method for quasiplanar neutron-focusing supermirrors on metal substrates. Based on the obtained results, research and development for neutron-focusing supermirrors should shift to axisymmetric forms. A restriction hindering the development of such axisymmetric mirrors is the supermirror deposition; as the supermirror neutron reflectivity is dependent on the precise control of the thickness, excessive curvature is unacceptable. However, in a recent breakthrough at the ion-beam sputtering facility at KURNS, a sputtering machine with a rocking mechanism realized the deposition of functioning supermirrors on curved surfaces up to $\pm 10^\circ$. With this sputtering machine, supermirrors on partial ellipsoids were realized [18], which are currently being used as phase-correction devices for neutron resonance spin echo spectrometers [19]. This indicates that the design possibilities for focusing supermirrors are expanding; thus, the development of associated technologies for substrate preparation must be propelled.

Further, this development should lead to the ultimate form of neutron-focusing supermirrors: a self-standing axisymmetric supermirror shell similar to the Wolter optics for X-rays. Applications of such neutron-focusing mirrors are in progress using nickel mirrors [20]; however, supermirrors with similar form are awaited. Our techniques for the figuring and polishing of metal substrates can contribute to such development in future, e.g., in preparing precise mandrels for the supermirrors.

6. Conclusion

A working neutron-focusing supermirror assembly was developed on metal substrates for neutron reflectometer SOFIA at BL16 in J-PARC MLF. The supermirror demonstrated satisfactory focusing performance for SOFIA by converging the neutrons to a Gaussian distribution with an FWHM of 0.13 mm. This performance was enabled by reducing the waviness and surface roughness of the substrates. With the focusing supermirror, the illumination of small samples was intensified in SOFIA, improving the efficiency of the beam time. The results on the improved neutron reflectometry will be reported in our future work.

Funding

Photon and Quantum Basic Research Coordinated Development ProgramMinistry of Education, Culture, Sports, Science and Technology; Adaptable and Seamless Technology Transfer Program through Target driven R & D (A-STEP); Japan Science and Technology Agency.

Acknowledgments

Neutron measurements were performed on BL16 at the Materials and Life Science Facility, J-PARC, Japan, under program nos. 2014S08 and 2019I1601. The supermirror coating was carried out in part under the Visiting Researcher's Program of KURNS.

References

1. N. Torikai, N. L. Yamada, H. Sagehashi, T. Sugita, S. Goko, M. Furusaka, Y. Higashi, M. Hino, T. Fujiwara, and H. Takahashi, "Development of a physically bent cylindroid mirror for beam focusing for a pulsed neutron reflectometer," *IOP Conf. Ser.: Mater. Sci. Eng.* **24**, 012016 (2011).
2. S. Mühlbauer, P. Niklowitz, M. Stadlbauer, R. Georgii, P. Link, J. Stahn, and P. Böni, "Elliptic neutron guides—focusing on tiny samples," *Nucl. Instrum. Methods Phys. Res., Sect. A* **586**(1), 77–80 (2008).
3. E. Rantsiou, T. Panzner, P. Hautle, and U. Filges, "Using parabolic supermirror lenses to focus and de-focus a neutron beam," *J. Phys.: Conf. Ser.* **528**, 012009 (2014).
4. G. E. Ice, J.-Y. Choi, P. Z. Takacs, A. Khounsary, Y. Puzyrev, J. J. Molaison, C. A. Tulk, K. H. Andersen, and T. Bigault, "Nested neutron microfocusing optics on SNAP," *Appl. Phys. A* **99**(3), 635–639 (2010).
5. G. G. Simeoni, R. G. Valicu, G. Borchert, P. Böni, N. G. Rasmussen, F. Yang, T. Kordel, D. Holland-Moritz, F. Kargl, and A. Meyer, "Focusing adaptive-optics for neutron spectroscopy at extreme conditions," *Appl. Phys. Lett.* **107**(24), 243503 (2015).
6. N. Rasmussen, G. Simeoni, and K. Lefmann, "Optimizing a neutron-beam focusing device for the direct geometry time-of-flight spectrometer toftof at the frm ii reactor source," *Nucl. Instrum. Methods Phys. Res., Sect. A* **816**, 106–112 (2016).
7. M. Yamada, U. Filges, T. Hosobata, Y. Yamagata, and E. Rantsiou, "Adaptive focusing optics for extreme conditions," *J. Neutron Res.* **20**(4), 113–116 (2019).
8. M. Nagano, F. Yamaga, N. Zettsu, D. Yamazaki, R. Maruyama, K. Soyama, and K. Yamamura, "Development of fabrication process for aspherical neutron focusing mirror using numerically controlled local wet etching with low-pressure polishing," *Nucl. Instrum. Methods Phys. Res., Sect. A* **634**(1), S112–S116 (2011).
9. M. Nagano, F. Yamaga, D. Yamazaki, R. Maruyama, H. Hayashida, K. Soyama, and K. Yamamura, "High-precision figured thin supermirror substrates for multiple neutron focusing device," *J. Phys.: Conf. Ser.* **340**, 012016 (2012).
10. K. Yamamura, M. Nagano, H. Takai, N. Zettsu, D. Yamazaki, R. Maruyama, K. Soyama, and S. Shimada, "Figuring of plano-elliptical neutron focusing mirror by local wet etching," *Opt. Express* **17**(8), 6414–6420 (2009).
11. S. Takeda, Y. Yamagata, N. L. Yamada, M. Hino, T. Hosobata, J. Guo, S. Morita, T. Oda, and M. Furusaka, "Development of a large plano-elliptical neutron-focusing supermirror with metallic substrates," *Opt. Express* **24**(12), 12478–12488 (2016).
12. T. Hosobata, N. L. Yamada, M. Hino, Y. Yamagata, T. Kawai, H. Yoshinaga, K. Hori, M. Takeda, S. Takeda, and S. Morita, "Development of precision elliptic neutron-focusing supermirror," *Opt. Express* **25**(17), 20012–20024 (2017).
13. N. L. Yamada, N. Torikai, K. Mitamura, H. Sagehashi, S. Sato, H. Seto, T. Sugita, S. Goko, M. Furusaka, T. Oda, M. Hino, T. Fujiwara, H. Takahashi, and A. Takahara, "Design and performance of horizontal-type neutron reflectometer SOFIA at J-PARC/MLF," *Eur. Phys. J. Plus* **126**(11), 108 (2011).
14. K. Mitamura, N. L. Yamada, H. Sagehashi, N. Torikai, H. Arita, M. Terada, M. Kobayashi, S. Sato, H. Seto, S. Goko, M. Furusaka, T. Oda, M. Hino, H. Jinnai, and A. Takahara, "Novel neutron reflectometer SOFIA at J-PARC/MLF for in-situ soft-interface characterization," *Polym. J.* **45**(1), 100–108 (2013).
15. J. Stahn and A. Glavic, "Focusing neutron reflectometry: Implementation and experience on the TOF-reflectometer Amor," *Nucl. Instrum. Methods Phys. Res., Sect. A* **821**, 44–54 (2016).
16. C. Klausler, R. Bergmann, U. Filges, and J. Stahn, "A selene guide for AMOR," *J. Phys.: Conf. Ser.* **1021**, 012024 (2018).
17. M. Hino, T. Oda, M. Kitaguchi, N. L. Yamada, S. Tasaki, and Y. Kawabata, "The ion beam sputtering facility at KURRI: Coatings for advanced neutron optical devices," *Nucl. Instrum. Methods Phys. Res., Sect. A* **797**, 265–270 (2015).
18. T. Hosobata, M. Hino, H. Yoshinaga, T. Kawai, H. Endo, Y. Yamagata, N. L. Yamada, and S. Takeda, "Precision Mechanical Design of 900 mm Long Ellipsoidal Neutron-focusing Supermirror for VIN ROSE at J-PARC/MLF," *JPS Conf. Proc.* **22**, 011010 (2018).
19. H. Endo, T. Oda, M. Hino, and T. Hosobata, "Current status of the neutron resonance spin echo spectrometer on BL06 ‘VIN ROSE’ at MLF, J-PARC," *Phys. B* **564**, 91–93 (2019).
20. D. S. Hussey, H. Wen, H. Wu, T. R. Gentile, W. Chen, D. L. Jacobson, J. M. LaManna, and B. Khaykovich, "Demonstration of focusing wolter mirrors for neutron phase and magnetic imaging," *J. Imaging* **4**(3), 50 (2018).